The effect of aerosol microstructure on the error in estimating wind velocity with a Doppler lidar

V.A. Banakh, Ch. Werner,* and I.N. Smalikho

Institute of Atmospheric Optics,
Siberian Branch of the Russian Academy of Sciences, Tomsk
** German Aerospace Center, Oberpfafenhofen, Germany*

Received May 3, 2000

The paper describes the investigation into the use of the effect of aerosol microstructure on the error in estimating wind velocity using a cw CO_2-laser Doppler lidar. It has been shown, based on the numerical simulation of a lidar return, that aerosol particles make essentially different contributions, due to different sizes, to a measured lidar return that may cause the deviation of the lidar return statistics from the Gaussian one thus resulting in the increase of the error in lidar estimation of wind velocity, especially at small volumes sounded with the lidar. With the increase of the efficient volume sounded the error in estimation of the wind velocity decreases.

Introduction

The Doppler lidar return power spectrum enables one to assess the velocity of motion of scattering aerosol particles. At a sufficiently large number of particles in the scattering volume and taking account complete entrainment of particles by a turbulent airflow, the obtained estimate of the velocity V_D can be considered as the radial component of wind velocity $\bar{V}_r$ averaged over the scattering volume sounded.[1–4] However, in reality, V_D differs from $\bar{V}_r$ by a certain random value V_e that determines the error of the radial velocity estimate. The traditional approach to the investigation of the error V_e is based on an assumption of Gaussian statistics of the Doppler lidar return.[3–6] However, in the case of a cw Doppler lidar, when an effective scattering volume is formed by focusing the sounding beam so that the beam size varies with the range of sounding, this approach does not always provides for correct interpretation of the experimental data, especially in the case of small scattering volumes. In the atmosphere the aerosol particles moving at different velocities due to difference in their sizes make essentially different contribution to measured lidar return that may cause the deviation of the lidar return statistics from the Gaussian one and may result in a different level of error V_e.

This paper analyzes the error in estimating the wind velocity from data of a cw Doppler lidar taking into account the aerosol microstructure.

1. Determination of the measurement error in wind velocity from time spectrum

The estimate of the radial component of wind velocity $V_D(t)$, obtained from the Doppler lidar return power spectrum measured at an instant of time t can be presented in the following form[7,8]:

$$V_D(t) = \bar{V}_r(t) + V_e(t) , \qquad (1)$$

where

$$\bar{V}_r(t) = \int_0^\infty dz\, Q_s(z)\, V_r(z, t) \qquad (2)$$

is the radial wind velocity averaged over scattering volume (the integration is made along the axis of the laser beam propagation z of the Cartesian coordinate system $\mathbf{r} = \{z, x, y\}$, $Q_s(z)$ is the weighting function characterizing the sounding range and the effective longitudinal size of the scattering volume (spatial resolution). Under the condition $ka_0^2 \gg R$ ($k = 2\pi/\lambda$, where λ is the wavelength, a_0 is the initial radius, and R is the focal length of a sounding beam) the function $Q_s(z)$ is described by the formula:

$$Q_s(z) = \{\pi k a_0^2 [(1 - z/R)^2 + z^2/(ka_0^2)]\}^{-1}. \qquad (3)$$

The component $V_e(t)$ in Eq. (1) is the error in the velocity estimate, i.e., the random deviation of the estimate V_D from a radial wind velocity averaged over the sounding volume $\bar{V}_r$. For obtaining unbiased estimate of the velocity, when $\langle V_D \rangle = \langle V_r \rangle$, one has to have that $\langle V_e \rangle = 0$, where the angular brackets denote the averaging over the ensemble of realizations. The level of V_e fluctuations is indicative of the correlation between the velocity measured with the Doppler lidar and the radial component of the actual wind velocity averaged over the volume sounded. In the general case, the quantity V_e is conditioned by the random temporal variations of the field of scattered wave and by noise in the system. The measured components of the "unsmoothed" Doppler power spectrum of lidar return with the frequency resolution Δf undergoes strong fluctuations. In this case the error in the velocity

0235-6880/00/08 685-07 $02.00

estimated with the Doppler formula $V_D = (\lambda/2)f_D$, where f_D is the frequency, which accounts for the "center of gravity" of spectral distribution, may be essential. To decrease the Doppler spectrum fluctuations and, correspondingly, to reduce the error in the velocity estimation, f_D is estimated after averaging over N "unsmoothed" spectra. It is evident that with the increase of time of integration in measuring the spectrum $t_0 = N/\Delta f$, the level of V_D fluctuations must decrease.

Since $\bar{V}_r(t)$ is a random value, i.e., it varies from measurement to measurement unpredictably, it is impossible to determine $V_e(t)$ directly from the estimate of $V_D(t)$. This raises the question on determination of the variance of the error of the velocity estimate $\sigma_e^2 = \langle V_e^2 \rangle$. In the Ref. 3 it was shown that $\bar{V}_r(t)$ and $V_e(t)$ are statistically independent.

Besides, $V_e(t_k)$ and $V_e(t_l)$ are the errors of the velocity estimates from different Doppler spectra ($t_k \neq t_l$), which do not correlate. This makes it possible, with the use of the results of Ref. 2 and with the assumption of the fulfillment of the hypothesis of the "frozen" turbulence, to obtain[7,8] the formula for the single-sided ($f \geq 0$) spectral density of the velocity fluctuations measured with a Doppler lidar

$$S_D(f) = 2 \int_{-\infty}^{+\infty} d\tau \, \langle V'_D(t+\tau) \, V'_D(t) \rangle \, e^{-j2\pi f\tau}$$

in the following form

$$S_D(f) = S_z(f) \, H(f) + S_e. \qquad (4)$$

In Eq. (4) $V'_D = V_D - \langle V_D \rangle$, $0 \leq f \leq 1/(2t_0)$, $S_z(f)$ is the time spectrum of radial component of wind velocity at a fixed point of space ($z = R$) being described at the frequencies $f \gg U/L_V$ (L_V is the outer scale of turbulence) by the Kolmogorov–Obukhov law:

$$S_z(f) = 0.075 C_K \left(1 + \frac{1}{3}\sin 2\gamma\right) \varepsilon^{2/3} U^{2/3} f^{-5/3}, \quad (5)$$

where $C_K \approx 2$ is the Kolmogorov constant; $\gamma = \arccos(\langle V_r \rangle / U)$ is the angle between the wind direction and the sounding beam axis z; $U = |\langle \mathbf{V} \rangle|$ is the mean wind velocity; ε is the turbulent energy dissipation rate;

$$H(f) = 0.82 \left(1 + \frac{1}{3}\sin^2\gamma\right)^{-1} \int_{-\infty}^{+\infty} d\xi (1+\xi^2)^{-4/3} \times$$

$$\times \left[1 - \frac{8}{11} \frac{(\cos\gamma - \xi \sin\gamma)^2}{1+\xi^2}\right] \times$$

$$\times \exp\left(-\frac{4\Delta z \, f}{U} |\cos\gamma - \xi \sin\gamma|\right) \qquad (6)$$

is the transmission function of the low-frequency filter determining the spatial averaging over the sounding volume;

$$\Delta z = \frac{\lambda}{2} (R/a_0)^2 \qquad (7)$$

is the longitudinal size of the volume sounded;

$$S_e = 2\sigma_e^2 \, t_0 \qquad (8)$$

is the noise spectral component connected with the error $V_e(t)$ where t_0 is the time of measurement of a single Doppler spectrum of the lidar return power (t_0^{-1} is the data reading frequency).

Thus, using Eqs. (4)–(8) we can determine, from the measurements of the power spectrum $S_D(f)$, the dissipation rate of turbulent energy ε and the variance of the error σ_e^2. In this case, as a rule, at high frequencies the first component in Eq. (5) is less than S_e by more than one order of magnitude. For example, Figure 1 shows in the form of points two velocity spectra measured with a Doppler lidar at different Δz values.

The technique of calculating ε and σ_e^2 from the measurement data on $S_D(f)$ was described in Refs. 7 and 8. Note that although the values of σ_e, obtained from the experiment in the case of large signal-to-noise ratios, are small as compared with the Doppler spectrum width σ_s ($\sigma_e \sim 10^{-1}$–10^{-2} m/s), the error V_e is in some cases an essential interfering factor when estimating ε from the spectrum of $S_D(f)$, especially at narrow width of inertial interval and at large Δz.

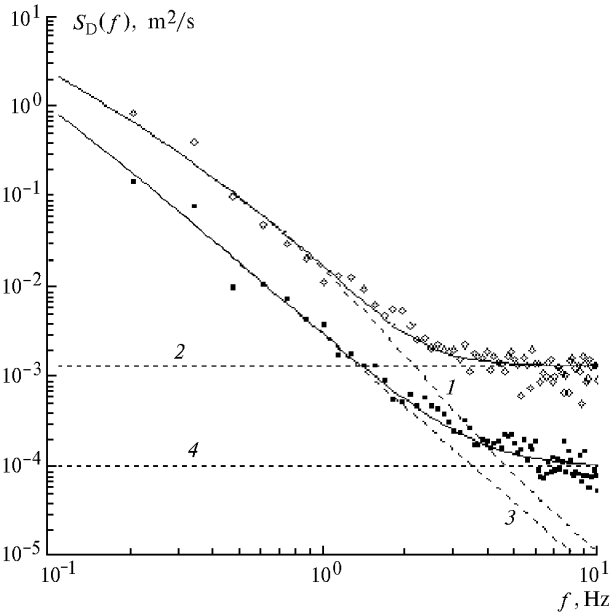

Fig. 1. Time spectra of wind velocity measured with a Doppler lidar at $\Delta z = 2.3$ m and $\Delta z = 100$ m: the experimental data are presented by rhombs ($\Delta z = 2.3$ m) and squares ($\Delta z = 100$ m); solid curves present the result of fitting by the formula (4) to the corresponding experimental dependences of the spectrum on frequency; dashed curves *1* and *3* show the calculations by the formula (*4*) at $S_e = 0$; dashed lines *2* and *4* denote the values of S_e.

In most of our field experiments made using the Doppler lidar of the German Aerospace Center the signal-to-noise ratio was large enough, so that the influence of system noise on the accuracy of the

velocity estimation can be neglected. Therefore, in the subsequent analysis of σ_e the noise will not be considered. To calculate the variance σ_e^2, we first use an assumption that the probability density of the Doppler lidar return obeys the Gaussian law.

2. The error of the velocity estimation under the assumption of Gaussian statistics of lidar returns

If the amplitudes of scattering by aerosol particles were the same, the one-dimensional probability density of a lidar return would be close to the Gaussian one even if only ten particles were present in the volume sounded. However, the velocities of the particles' motion, entrained by a turbulent flux, will correlate only within the limits of the outer scale of turbulence L_V (that can be much larger than Δz).

Therefore, the two-dimensional probability density of a lidar return (whose arguments are the lidar returns recorded at different moments in time) will differ from the two-dimensional Gaussian distribution.[9] Nevertheless, using the Gaussian model for the lidar return the two-dimensional probability density (TDPD) we can obtain, assuming that the condition $\lambda\Delta f/(2\sigma_s) \ll 1$ holds, a simple expression for the variance of the velocity estimation error $\sigma_e^2 = \sigma_{en}^2$ (here the index n denotes the use of the Gaussian model for the TDPD) in the form[5,6]

$$\sigma_{en}^2 = \frac{1}{8\sqrt{\pi}} \frac{\lambda}{t_0} \sigma_s, \qquad (9)$$

where at $ka_0^2 \gg R$ and $\Delta z \ll L_V$ the mean square of the Doppler spectrum width[2]

$$\sigma_s^2 = C_K(2/\pi)^{2/3}(\varepsilon\Delta z)^{2/3}, \qquad (10)$$

and at $\Delta z \gg L_V$ the value of $\sigma_s^2 = \sigma_V^2 = \langle[V_r - \langle V_r\rangle^2]^2\rangle$.

Really, when the size of the sounded volume Δz far exceeds the turbulence outer scale L_V, the TDPD is Gaussian and Eq. (9) accurately describes the estimate error of mean velocity of particle's motion in the volume sounded provided that the particles have same sizes. Moreover, as the comparison with the results of numerical simulation indicates, when the scattering particles have same sizes, Eq. (9) yields correct estimates of the error at $\Delta z \ll L_V$.[10,11]

At the same time, the experimental values of σ_e are essentially different than the estimates of σ_e by formula (9). The experiments were made under various turbulent conditions (different ε) and $\Delta z \ll L_V$. From the time spectra of wind velocity measured with the Doppler lidar we determined the errors σ_e and using Eq. (9) the value of σ_{en} was calculated where σ_s was estimated from the corresponding experimental data. The ratios σ_e/σ_{en} at different σ_s are plotted in Fig. 2.

From Fig. 2 it follows that on the average σ_e exceeds σ_{en} approximately by one order of magnitude.

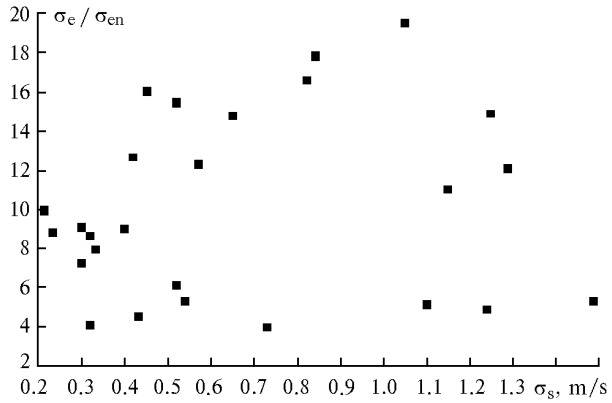

Fig. 2. The experimental values of the ratio σ_e/σ_{en} obtained at different σ_s.

At small-size sounding volume, when $\Delta z \ll L_V$ according to Eqs. (9), (10), and (7) $\sigma_{en}^2 \sim R^{2/3}$, i.e., with the increasing sounding range (the size of the sounding volume) the variance of the error in the case of the Gaussian statistics of the lidar return must grow. However, as one can see, in particular, from Fig. 1 and other experimental data (cited below), the error in the estimate decreases with the increasing R. To explain the difference between the behavior of σ_e and σ_{en}, we must take into account the effect of aerosol particle microstructure on the statistical properties of scattered light.

3. Account for the scattering particles microstructure. Numerical simulation

Let the useful component of the Doppler lidar return $j_s(t)$ be presented in the following complex form[8]:

$$j_s(t) = \frac{2\eta e}{h\nu}\sqrt{\frac{P_L}{P_T}}\,\lambda \sum_{i=1}^{n_s} A_s(a_i)E^2(\mathbf{r}_i(t)) \times \exp[j\Psi_i + j\,2kV_r(z_i)t], \qquad (11)$$

where η is the detector quantum efficiency; e is the electron charge; $h\nu$ is the photon energy; P_L and P_T denote the power of the reference and sounding beams, respectively. $A_s(a_i)$ is the amplitude of scattering by ith particle with the dimensions of a_i,

$$E(\mathbf{r}) = \frac{\sqrt{P_T/\pi}}{a_0\, g(z)} \exp\left[-\left(1 + j\frac{k\,a_0^2}{R}\right)\frac{\rho^2}{2\,a_0^2\,g(z)}\right]$$

is the complex amplitude of the sounding beam wave; $g(z) = (1 - z/R) + jz(ka_0^2)$; $\rho = \{x, y\}$; $\Psi_i = 2kz_i$ is the initial phase of the wave scattered by the ith particle; $\mathbf{r}_i(t) = \mathbf{r}_i + t\mathbf{V}(\mathbf{r}_i)$ is the coordinate of the ith particle at the moment t in time; n_s is the number of scattering particles.

From Eq. (11) and taking into account the statistical independence of the phases Ψ_i one can obtain

an expression for the mean lidar return power $S = \langle |j_s(t)|^2 \rangle / 2$ in the following form:

$$S = \frac{1}{2}\left(\frac{2\eta e}{h\nu}\right)^2 \frac{P_L}{P_T}\,\lambda^2\,\frac{1}{4\pi}\,\langle\sigma\rangle\,\rho_0\,V_{\text{eff}}\,|\,E(\mathbf{r}_{\max})\,|^4, \quad (12)$$

where

$$\langle\sigma\rangle = \int_0^\infty da\;\sigma(a)\,f(a) \quad (13)$$

is the mean value of the backscattering cross section; $\sigma(a) = 4\pi A_s^2(a)$ is the backscattering cross section of a particle of size a; $f(a)$ is the particle size-distribution function; ρ_0 is the particle concentration;

$$V_{\text{eff}} = \int_0^\infty dz \int_{-\infty}^\infty d^2\rho\;|\,E(\mathbf{r})\,|^4 / |\,E(\mathbf{r}_{\max})\,|^4 \quad (14)$$

is the efficient sounding volume; $|E(\mathbf{r}_{\max})|^4 = (\pi/\lambda)^2 \times P_T^2/V_{\text{eff}}$, $\mathbf{r}_{\max} = \{z_{\max}, 0\}$ is the coordinate of the $|E(\mathbf{r})|^4$ function maximum, $z_{\max} = R/[1 + (R/ka_0^2)^2]$. At $ka_0^2 \gg R$ we have from Eq. (14):

$$V_{\text{eff}} = \frac{\lambda^3}{16\pi}\,\frac{R^4}{a_0^4}\,, \quad (15)$$

and formula (12) for S reduces to the expression obtained in Ref. 12:

$$S = \frac{1}{2}\left(\frac{\eta e}{h\nu}\right)^2 P_L P_T\,\lambda\beta_\pi, \quad (16)$$

where $\beta_\pi = \rho_0\langle\sigma\rangle$ is the coefficient of backscattering.

Now we introduce the parameter $\rho_c(a)$ presenting the concentration of particles with the size exceeding a

$$\rho_c(a) = \rho_0 \int_a^\infty da'\,f(a'), \quad (17)$$

where the particle concentration $\rho_c(0) = \rho_0$ if one accounts for the normalization $\int_0^\infty da\,f(a) = 1$. For the particle size-distribution function we have from Eq. (17) that

$$f(a) = -\frac{1}{\rho_0}\,\frac{d\rho_c(a)}{da}\,. \quad (18)$$

To simulate random realizations of the particle size, we approximated the empirical model $\rho_c(a)$, taken from Ref. 13, by a simple formula

$$\rho_c(a) = \frac{\rho_0}{1 + \alpha_1 a^3}, \quad (19)$$

where $\rho_0 = 1430\ \text{cm}^{-1}$ and $\alpha_1 = 7.15\cdot10^3\ \mu\text{m}^{-3}$.

Assuming that all particles are spherical and have the same complex refractive index $m = n + j\kappa$ of the particulate matter, we calculated the backscattering cross sections using the Mie theory.[14] For m we used the model proposed in Ref. 13 assuming the wavelength $\lambda = 10.6\ \mu\text{m}$.

The mean number of particles in the sounding volume is defined by the formula $N_P = \rho_0 V_{\text{eff}}$. However, the scattering particles, depending on their size, can have different optical activity. Therefore, there exists an effective concentration ρ_{eff} of the largest particles that make the main contribution to the backscattering coefficient β_π. Now we determine the value of $\rho_{\text{eff}} = \rho_c(a_m)$, where a_m is the particle size obtained from the solution of the following equation:

$$\int_0^{a_m} da\;\sigma(a)f(a) \Big/ \int_0^\infty da\;\sigma(a)f(a) = 0.1, \quad (20)$$

i.e., we consider that the particles with sizes $a > a_m$ make a 90% contribution to the mean signal power S. From calculations we obtained that $a_m = 0.97\ \mu\text{m}$, $\rho_{\text{eff}} = 0.22\ \text{cm}^{-3}$.

By analogy with N_P we determine the number of effectively scattering particles to be N_{eff} as $N_{\text{eff}} = \rho_{\text{eff}} \cdot V_{\text{eff}}$. Then for the lidar operated at $\lambda = 10.6\ \mu\text{m}$ and $a_0 = 7.5\ \text{cm}$ and a selected model of aerosol we have:

1) at $R = 50$ m $V_{\text{eff}} = 4.7\ \text{cm}^3$, $N_P \approx 6.7\cdot10^3$, $N_{\text{eff}} \approx 1$;

2) at $R = 100$ m $V_{\text{eff}} = 74.9\ \text{cm}^3$, $N_P \approx 10^5$, $N_{\text{eff}} \approx 16$;

3) at $R = 500$ m $V_{\text{eff}} = 4.7\cdot10^4\ \text{cm}^3$, $N_P \approx 6.7\cdot10^7$ and $N_{\text{eff}} \approx 10^4$.

It is evident from the above examples that at $R = 50$ m, in spite of a large total number of all particles in a volume sounded N_P, $N_{\text{eff}} \approx 1$ and, hence, the one-dimensional lidar return probability density will differ from the Gaussian one. On the contrary, at $R = 500$ m, the number N_{eff} is very large and the lidar return must obey the Gaussian statistics.

To investigate the influence of aerosol microstructure on the accuracy of Doppler estimates of the wind velocity we used numerical simulation of the lidar return $j_s(t)$. The sounding path was divided into layers, and within each layer random values of the backscattering amplitude $A(a_i)$ were simulated as well as the initial phases Ψ_i and radial velocities of the particles $V_r(z_i)$ fully entrained by a turbulent airflow (within an isolated layer the values V_r were interpreted to be the same for all particles entrained). The particle removal out from the volume sounded by the side wind was also considered for. A detailed description of the simulation algorithm can be found in Ref. 11.

Using the simulated realizations of $j_s(t)$ ($t \in [0, t_0]$) we calculated the lidar return power spectra of $W(f)$ with the frequency resolution $\Delta f = 20$ kHz. Then using thus obtained spectra $W(f)$ we estimated V_D and according to the difference between V_D and the radial velocity $\bar{V}_r$ averaged over sounding volume the random error V_e was determined. The variance σ_e^2 was calculated, as minimum, from 300 realizations.

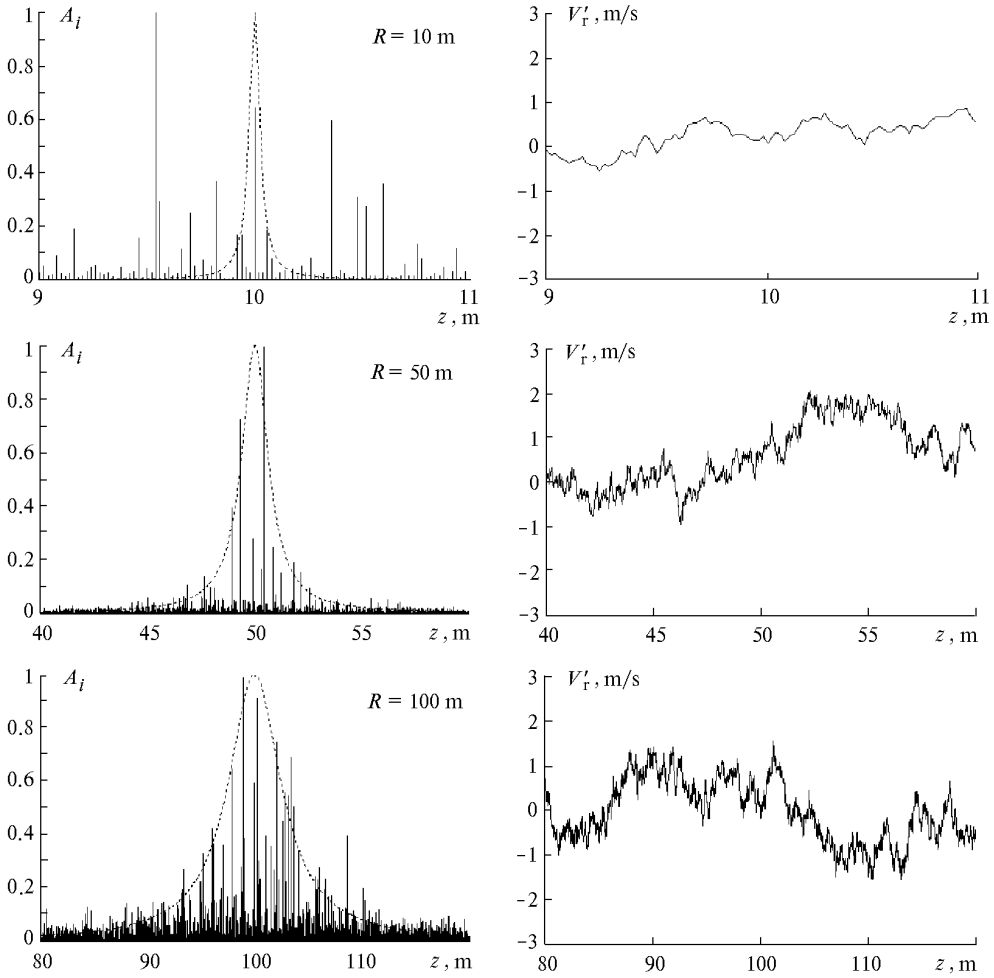

Fig. 3. Examples of simulation of instantaneous distributions of amplitudes A_i and fluctuations of the radial velocity V'_r along the z axis.

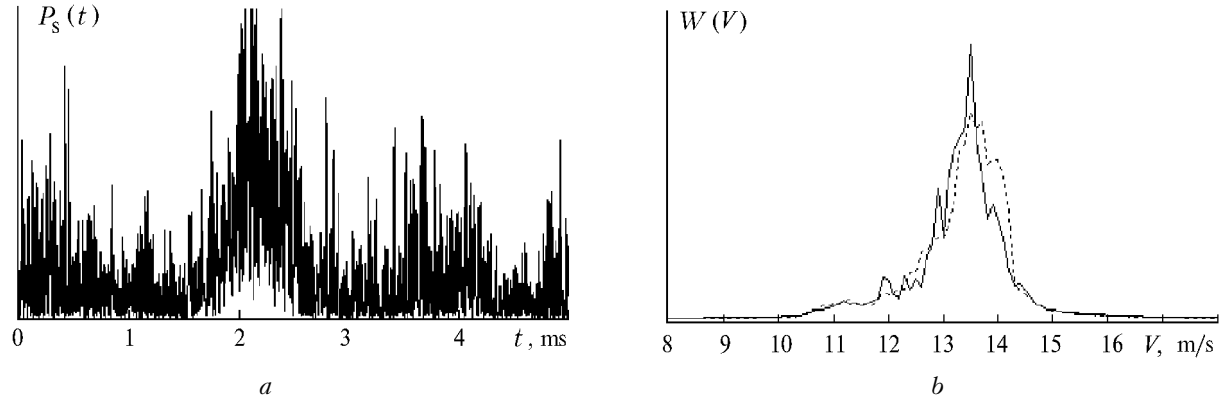

Fig. 4. An example of simulation of the dependence of lidar return power P_s on time t (*a*) and the Doppler spectrum estimation from the simulated lidar return (solid curve) (*b*); dashed curve denotes the spectrum obtained from the data simulated under conditions of equal scattering amplitudes for all particles, R = 50 m (Δz = 2.3 m); σ_V = 1.5 m/s; L_V = 50 m.

Figure 3 shows the examples of simulation of instantaneous distribution (along the z axis) of the amplitudes showing the contribution to the lidar return $j_s = \sum_i A_i \, e^{j\Psi i}$ from the ith layer (the left-hand panels) and the turbulent fluctuations of radial wind velocity $V'_r = V_r - \langle V_r \rangle$ (the right-hand panels) at the layer thickness l = 2 cm. Solid curves in the figures for A_i show the corresponding normalized distributions of

$Q_s(z)$. It is evident that at very small scattering volume sounded (when $R = 10$ m) the maximum amplitude A may be spaced at a large, as compared with $\Delta z \approx 9$ cm, distance from the center of the volume $z = R$. Such a situation is possible only with the appearance, within the beam limits (but outside the interval $[R - \Delta z/2, R + \Delta z/2]$), of one large particle. In this case, the particle velocity can strongly differ from V_r (see the figure for V_r').

The effect of one large particle on the lidar return is demonstrated in Fig. 4, where the left-hand panel shows an example of simulation of the instantaneous lidar return power $P_s(t) = |j_s(t)|^2/2$, which manifests itself as the peak of ~1-ms width determined by the time of this particle travel across the sounding beam in the vicinity of a focused beam waist $z \in [R - \Delta z/2, R + \Delta z/2]$. The right-hand panel shows, by the solid line, the spectrum $W(V)$ of Doppler lidar return ($V = (\lambda/2)f$) calculated from the simulated relationship $j_s(t)$ is given. The spectrum $W(V)$ is shown by the dashed curve. This spectrum was obtained assuming the amplitudes of backscattering from all particles to be the same and at the same realization of $V_r(z)$, used for the case of polydisperse aerosol. A typical $P_s(t)$ dependence is observed in the field experiment at small size of sounding volume.[15]

4. Results of numerical and field experiments

The numerical simulation was used both for the case, when all particles have same size (the scattering amplitudes $A_s(a_i)$ for all the particles are the same), and for the case of polydisperse aerosol (the statistics of particle size a_i is described by the model (19)), but at one and the same total concentration of particles ρ_0. In the first case even at $R = 10$ m, when $V_{eff} = 7.5 \cdot 10^{-4}$ cm^{-3} and $\rho_0 = 1430$ cm^{-3} the number of particles in the volume sounded $N_P = N_{eff} = 11$, the statistics of lidar return will be close to the Gaussian one, and therefore the error in estimate of wind velocity assessed from the simulated data at $A_s(a_i) = \text{const}$ is denoted, by analogy with (9), as σ_{en}, and for the case of polydisperse aerosol it is denoted as σ_e. Figure 5 shows the dependence of the ratio σ_e/σ_{en} on R obtained from the data of numerical simulation. It is evident that the value σ_e can exceed σ_{en} by one order of magnitude as in the field experiment (see Fig. 2).

Field experiments were carried out during different days at various wind turbulence intensities in the atmospheric boundary layer. In all experiments the measurement time of a single Doppler spectrum $t_0 = 50$ ms. The minimum sounding range R was 50 m ($\Delta z \approx 2.3$ m). The aerosol microstructure parameters did not require close control, but rough estimates indicate that the aerosol concentration for different measurements could vary considerably. In this case the signal-to-noise ratio remained sufficiently high in order that the influence of system noise on the accuracy of wind velocity estimation could be ignored.

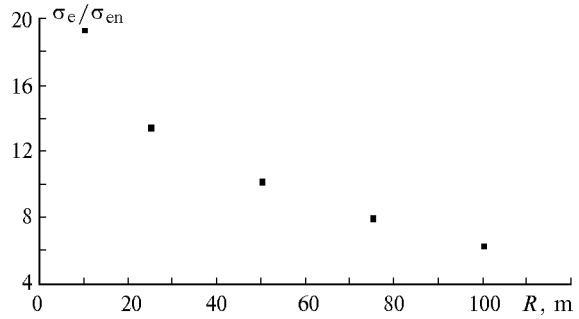

Fig. 5. The dependence of the ratio σ_e/σ_{en} on R calculated from data of numerical simulation.

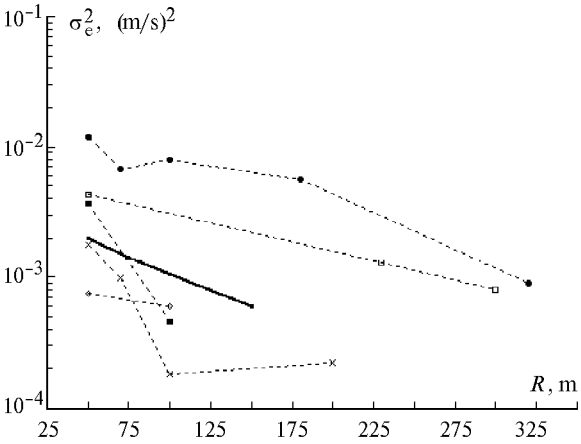

Fig. 6. The dependence of σ_e^2 on R; the dots connected by dashed lines denote the field experiment; solid curve is the numerical experiment.

Figure 6 shows the dependence of σ_e^2 on R. The values of σ_e^2, calculated from the measurement data, are denoted by dots connected by dashed lines, and the values of σ_e^2, calculated from the numerical simulation data, are denoted by solid curve. In contrast to the field experiment, where the σ_e^2 dependences on R were obtained under different conditions of dynamic turbulence, mean wind velocity and parameters of aerosol microstructure, the solid curve was calculated at one fixed value $\sigma_r = 1$ m/s (transverse component of the mean wind velocity $V_\perp = 4$ m/s) and one model for $\rho_c(a)$ given above. With the increase of R (and, respectively, the increase of $V_{eff} \sim R^4$) the number of particles in the volume sounded grows strongly that leads to a considerable increase of time of calculations. Therefore we managed to obtain the simulated dependence of σ_e^2 on R only up to $R = 150$ m. It follows from the figure that with the increase of the volume sounded the variance of σ_e^2 decreases. In this case, on the average, the behavior of σ_e^2, estimated from the data of field experiments, is similar to the behavior of σ_e^2 determined on the basis of numerical simulation.

Conclusion

In conclusion it may be stated that the experimental values of the error σ_e of the wind velocity estimate, on the average, exceed by one order of magnitude the theoretical values of the error σ_{en}, calculated under the assumption of Gaussian statistics of the lidar return. The values σ_e, calculated based on the numerical simulation with the account of aerosol microstructure, also exceed the value of σ_{en} by approximately one order of magnitude. The data of numerical and field experiments show that in contrast to σ_{en}, the error σ_e decreases with the increasing size of the volume sounded. Thus, the microstructure factor of a discrete scattering medium produces a decisive effect on the error σ_e in the wind velocity estimation.

Acknowledgments

The work was done under the support from the Russian Foundation for Basic Research (Grants No. 98–05–03131 and No. 00–05–64033).

References

1. V.A. Banakh, I.N. Smalikho, F. Köpp, and Ch. Werner, Appl. Opt. **34**, No. 12, 2055–2067 (1995).
2. I.N. Smalikho, Atmos. Oceanic Opt. **8**, No. 10, 788–793 (1995).
3. R. Frehlich, J. Atmos. Oceanic Technol. **14**, No. 2, 54–72 (1997).
4. V.A. Banakh and I.N. Smalikho, Atmos. Oceanic Opt. **10**, No. 12, 957–965 (1997).
5. R.J. Keeler, *First Topical Meeting on Coherent Laser Radar*, Aspen (Opt. Soc. Am., 1980), pp. WA 3–1–WA 3–4.
6. R.J. Keeler, R.J. Serafin, R.L. Schwiesow, D.H. Lenschov, J.M. Vaughan, and A.A. Woodfield, J. Atmos. Oceanic Technol. **4**, No. 3. 113–128 (1987).
7. V.A. Banakh, Ch. Werner, F. Köpp, and I.N. Smalikho, Atmos. Oceanic Opt. **10**, No. 3, 202–208 (1997).
8. V.A. Banakh, I.N. Smalikho, F. Köpp, and Ch. Werner, J. Atmos. Oceanic Technol. **16**, No. 7, 1044–1061 (1999).
9. B. Krosiniani, P. Di Porto, and M. Bertolotti, *Statistical Characteristics of Scattered Light* [Russian translation] (Nauka, Moscow, 1980) 206 p.
10. V.A. Banakh, I.N. Smalikho, and Ch. Werner, *Tenth Biennial Coherent Laser Radar Technology and Applications Conference*, Oregon (1999) pp. 132–135.
11. V.A. Banakh, I.N. Smalikho, and Ch. Werner, Appl. Opt. (2000) (to be published).
12. T.R. Lawrence, D.J. Wilson, C.E. Craver, I.P. Jones, R.M. Huffaker, and J.A. Tomson, Rev. Sci. Instrum. **43**, No. 3, 512–518 (1972).
13. G.M. Krekov and R.F. Rakhimov, *Optical Detection Model of Continental Aerosol* (Novosibirsk, Nauka, 1982), 197 pp.
14. A. Ishimaru, *Wave Propagation and Scattering in Random Media* (Academic Press, New York, 1978), Part 1.
15. R.M. Hardesty, R.J. Keeler, M.J. Post, and R.A. Richter, Appl. Opt. **20**, No. 21, 3763–3769.